Hydrophilic–hydrophobic two-component polymer networks: 2. Synthesis and characterization of poly(ethylene oxide)-*linked*-polybutadiene*

Martin Weber and Reimund Stadler
Institut für Makromolekulare Chemie, Hermann Staudinger Haus, Stefan Meier Strasse 31, D-7800 Freiburg, FRG
(Received 14 September 1987; accepted 26 November 1987)

Hydrophilic–hydrophobic two-component networks were prepared by reacting end-functionalized poly(ethylene oxides) with polybutadiene. The poly(ethylene oxide)-*linked*-polybutadiene two-component networks phase-separate even for very short polyether chain lengths. By transmission electron microscopy, a bicontinuous interpenetrating morphological structure was determined. Heat capacity analysis shows that the mobility of the polybutadiene is influenced by the polyether phase. The same result is obtained from stress–strain experiments. Analysis of the swelling data in different solvents (tetrahydrofuran, cyclohexane, water) show that the hydrophobic–hydrophilic balance in such two-component networks is altered by varying the crosslink density and the polyether chain lengths.

(Keywords: two-component networks; bicontinuous structure; hydrophilic–hydrophobic balance)

INTRODUCTION

Crosslinked multicomponent polymer systems such as interpenetrating networks (IPNs) and semi-IPNs are of increasing interest for applications requiring functional polymer systems[1,2]. Another topologically different multicomponent system is a poly(A)-*linked*-poly(B) two-component network, in which poly(A) is an end-functionalized macromolecular crosslinker for poly(B).

In the first paper of this series[3] we reported the synthesis of poly(ethylene oxide) telechelics with 1,2,4-triazoline-3,5-dione units as the highly reactive end groups. These reactive telechelics can be used to crosslink polybutadiene by an 'ene' reaction of the enophilic 1,2,4-triazoline-3,5-dione with the allylic groups of polybutadiene[4,5]. As a result, poly(ethylene oxide)-*linked*-polybutadiene (PEO-*l*-PB) two-component networks with a chain topology schematically shown in *Figure 1* are obtained. In such networks, two immiscible polymers—one hydrophilic and the other hydrophobic—are combined to form a multicomponent system whose properties may be varied by changing the composition, either by increasing the crosslink density at constant PEO chain length or varying the polyether chain length at constant crosslink density. As demonstrated in *Figure 1*, the structure of these systems is somewhat analogous to crown ethers and/or polymer-bound crown ethers. Thus, we are interested in the hydrophilic–hydrophobic balance of these two-component networks.

The behaviour towards aqueous media is governed by the tendency of the two polymers to phase-separate and by the resulting multiphase morphology.

In this paper the synthesis of PEO-*l*-PB two-component networks with average polyether chain length between 200 and 600 are described. The thermal properties and the stress–strain and swelling behaviour of the networks are discussed.

EXPERIMENTAL

Synthesis of the networks

Polybutadiene was synthesized by standard anionic polymerization (break-seal technique) in cyclohexane (s-BuLi): $M_n = 34\,000$, $M_w/M_n = 1.05$. The synthesis of the reactive crosslinkers α,ω-di[4,4′-(1′,2′,4′-triazoline-3′,5′-dione)phenylene]-poly(ethylene oxides) XX (where XX denotes the polyether chain length) has been reported in detail in the previous paper[3]. The two reactive telechelics used in this paper were synthesized starting from hydroxy-terminated PEO 200 and 600.

The crosslinking ene reaction was performed in homogeneous 5% tetrahydrofuran (THF) solutions. Because both components are readily soluble in THF, mixing of the polymers is favourable. However, if a high-molecular-weight polybutadiene ($M_n = 200\,000$) is used in combination with a reactive telechelic of molecular weight 4000, no network is formed[4], probably due to phase separation between the polymers even in semidilute solution.

The reaction (ene reaction) proceeds rapidly at room temperature due to the high reactivity of the 1,2,4-triazoline-3,5-dione groups[5–8]. The two network series are designated 200-*i* and 600-*i* ($i = 1$ to 5). Their compositions are given in *Table 1*. The weight fraction of the crosslinker varies between 0.07 and 0.25. The polybutadiene is always the major component.

Differential scanning calorimetry

Differential scanning calorimetry measurements were performed on a Perkin–Elmer DSC-7 instrument. While

* Dedicated to Professor H.-J. Cantow on the occasion of his 65th birthday

0032-3861/88/061071-08$03.00

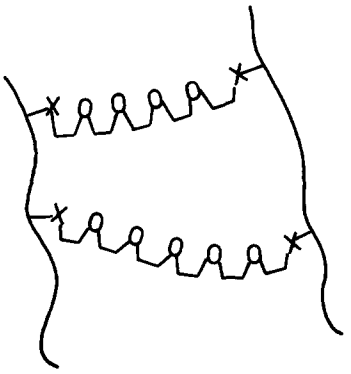

Figure 1 Schematic representation of a PEO-*l*-PB two-component network

Table 1 Compositions of network series 200-*i* and 600-*i*

Sample	Crosslinker (mol%)[a]	PB (wt%)	Crosslinker (wt%)	PEO (wt%)
200-1	0.65	92.81	7.19	3.2
200-2	0.87	90.66	9.34	4.21
200-3	1.09	88.59	11.41	5.14
200-4	1.32	86.60	13.40	6.01
200-5	1.75	82.91	17.09	7.69
600-1	0.74	88.54	11.46	7.19
600-2	0.98	85.37	14.63	9.18
600-3	1.24	82.18	17.82	11.17
600-4	1.48	79.38	20.62	12.95
600-5	1.98	74.22	25.78	16.20

[a] Per cent crosslinker per mole double bonds in PB

maintaining the block temperature at −180°C, measurements were performed from −130°C to +60°C at several heating rates (10, 20, 30 and 40 K min^{-1}). The glass transition temperatures were determined as the inflection points in the heat capacity changes, and the 'static glass transition temperature' was obtained by extrapolation to zero heating rate.

Stress–strain experiments

Stress–strain experiments were performed on an Instron 1122 tensile testing machine equipped with a microcomputer to record the stress and strain data directly. The machine was also equipped with a device for simultaneous birefringence measurements[9]. The parallel measured birefringence showed that all samples were optically homogeneous. No internal stresses were detected in the unstrained samples.

Swelling measurements

Strips of the samples (~ 50–100 mg) were immersed in a large excess of solvent. The degree of swelling was calculated assuming volume additivity from the weight increase, the density of the solvent and the density of the homopolymers. Swelling measurements were performed at 20, 30 and 40°C (±0.1°C).

RESULTS AND DISCUSSION

Differential scanning calorimetry

The two-component polymer networks consist of two inherently immiscible polymers: PB and PEO. These components are topologically linked together as shown in *Figure 1*. One important question is, whether a one-phase network is formed or whether phase separation occurs even for the short polyether chains used in this study? D.s.c. analysis helps to answer this question. However, the analysis of the glass transition behaviour may be complicated by the fact that, in crosslinked systems, the softening temperature increases with crosslink density as a consequence of reduced segmental mobility[10]. In the case of phase separation, two glass transition temperatures should be observed. Nevertheless, the amount of PEO in series 200-*i* may be too small to be detected by d.s.c. (*Table 1*).

Series 200-i. In *Figure 2* the d.s.c. traces for series 200-*i* at a heating rate of 40 K min^{-1} are shown. A distinct sharp glass transition corresponding to polybutadiene is detected for series 200-*i* at low temperatures. The transition temperatures, extrapolated to zero heating rate, are plotted in *Figure 3* as a function of the weight fraction of crosslinker.

The corresponding plot of the glass transition temperature as a function of crosslink density gives an approximately linear dependence. Both molecular mixing between the polybutadiene and the poly(ethylene oxide) and the increasing crosslink density could cause an increase in the glass transition temperature. At high heating rate (40 K min^{-1}) a second broad glass transition at approximately 290 K is observed for samples 200-2 to 200-5. With lower heating rates, this higher-temperature glass transition is difficult to localize. The temperature range over which this high-temperature glass transition occurs is about 50°C. The observation of this second glass transition shows that phase separation occurs even for the small polyether chains in series 200-*i*. Further information is available from the changes in heat capacity at the glass transition at low temperatures. *Table 2* summarizes the average heat capacity changes at $T_{g(low)}$. Comparison with the theoretically expected heat capacity change for the whole system (PB + PEO) shows that the experimental values are considerably smaller, even lower

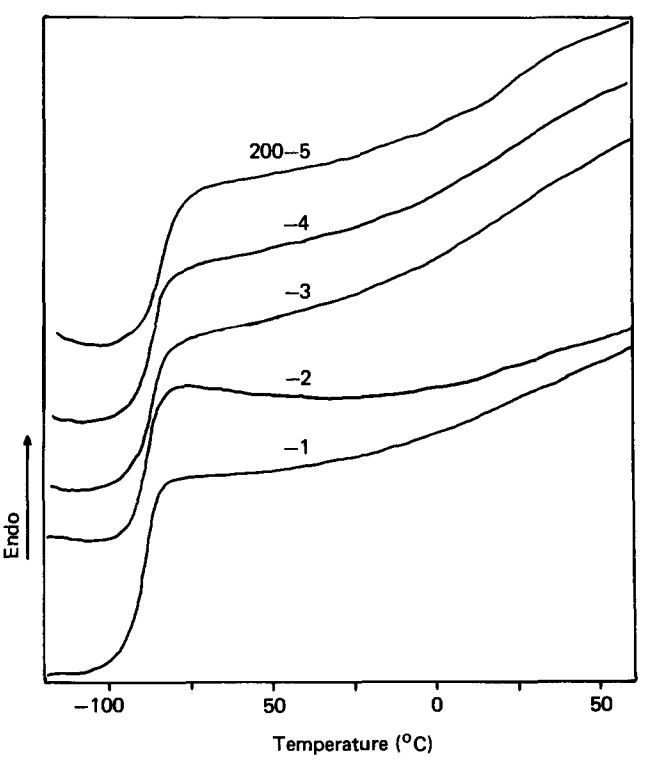

Figure 2 D.s.c. traces of network series 200-*i* (heating rate 40 K min^{-1})

than those expected for polybutadiene of similar microstructure alone[11]. Comparison of experimental and calculated values of the polybutadiene component shows that between 10 and 20% of the polybutadiene phase does not gain mobility at the low glass transition temperature. With this short polyether chain length, it is not possible to obtain quantitative data for the polyether transition. Nevertheless, the d.s.c. results show that no molecular mixing occurs in the networks with the low-molecular-weight polyether.

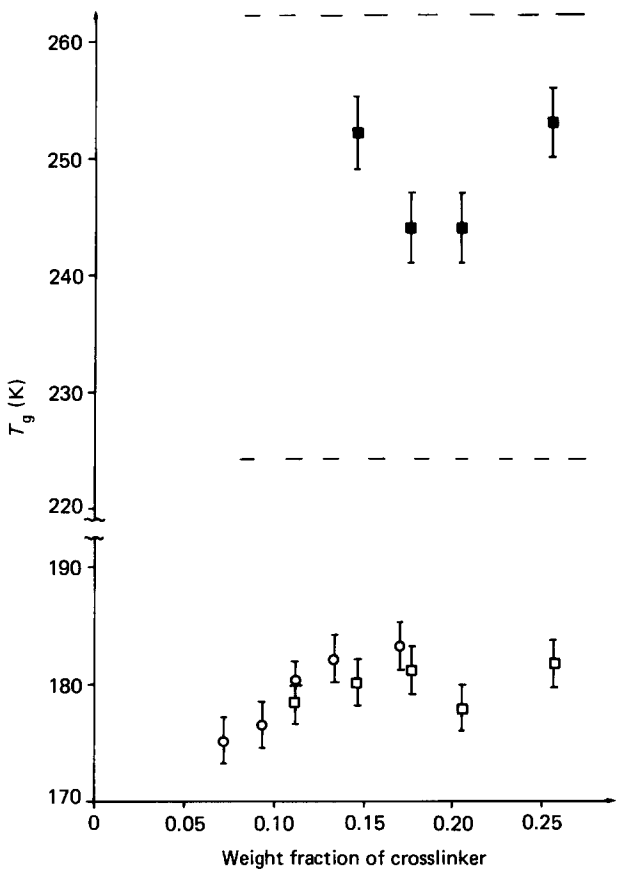

Figure 3 Dependence of the glass transition temperatures (extrapolated to zero heating rate) as a function of weight fraction of crosslinker: circles, series 200-*i*; squares, series 600-*i*; open symbols, PB transition; full symbols, PEO transition

Table 2 Results of the calorimetric measurements for series 200-*i*

Sample	T_g (PB) (K)	Δc_p ($J\,g^{-1}\,K^{-1}$)	Δc_p^{calc} ($J\,g^{-1}\,K^{-1}$)	Δc_p^{calc} (PB+PEO) ($J\,g^{-1}\,K^{-1}$)
200-1	175.2	0.479	0.494	0.557
200-2	176.5	0.448	0.483	0.565
200-3	179.9	0.428	0.472	0.572
200-4	182.2	0.433	0.461	0.579
200-5	183.2	0.461	0.441	0.591

Series 600-i. In the 600-*i* network series, i.e. longer PEO chains, two glass transitions are observed in all samples (*Figure 4*). As *Table 3* demonstrates, the lower-temperature glass transition does not vary with crosslink density. As in series 200-*i* this transition is quite sharp. A broader glass transition is also observed at higher temperatures with all samples. The breadth of this higher-temperature transition reduces with increasing polyether content. Nevertheless, the transition always covers at least 25 K. The transition temperatures extrapolated to zero heating rate are collected in *Table 3*. The data in *Figure 3* corresponding to the series 600-*i* polybutadiene glass transition show that the polybutadiene glass transitions are essentially independent of composition. This is indicative of a pure PB phase.

However, the slight dependence of the ether glass transition on composition demonstrates that the polybutadiene influences the polyether transition. In addition, it must be noted that at approximately 40°C above the polybutadiene T_g, far below the T_g of the polyether, a change in the slope of the heat capacity occurs, indicating the onset of additional heat-dispersing processes. *Table 3* also summarizes the experimental heat capacity values as well as the data calculated for polybutadiene and the polyether. Reasonable agreement between the calculated and experimental heat capacity changes at the T_g of the polyether is obtained. In contrast, the polybutadiene experimental heat capacity changes are as much as 25% lower than expected from composition data. The differences increase with increasing polyether content. This difference, however, can be accounted for by adding the heat capacity change observed prior to the polyether transition to that of the polybutadiene glass transition:

$$\Delta c_p(PB) + \Delta c_p(PB') = \Delta c_p^{calc}(PB)$$

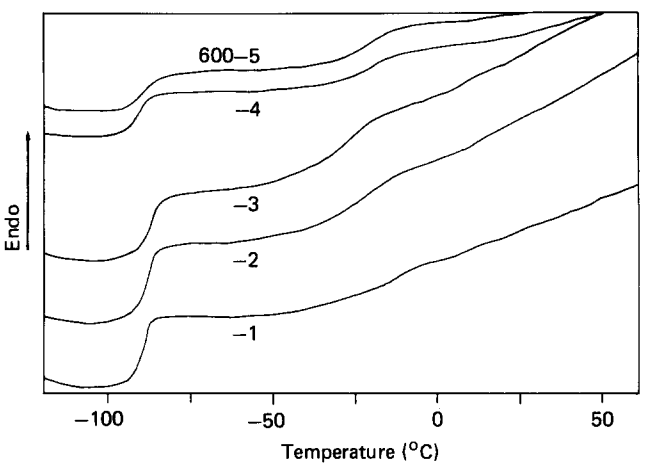

Figure 4 D.s.c. traces of network series 600-*i* (heating rate 40 K min^{-1})

Table 3 Results of the calorimetric measurements for series 600-*i*

Sample	T_g(PB) (K)	T_g(PEO) (K)	Δc_p(PB) ($J\,g^{-1}\,K^{-1}$)	Δc_p(PB')[a] ($J\,g^{-1}\,K^{-1}$)	Δc_p^{calc}(PB) ($J\,g^{-1}\,K^{-1}$)	Δc_p(PEO) ($J\,g^{-1}\,K^{-1}$)	Δc_p^{calc}(PEO) ($J\,g^{-1}\,K^{-1}$)
600-1	178.5		0.39	0.071	0.440	0.061	0.101
600-2	180.2	252.2	0.38	0.053	0.442	0.120	0.130
600-3	181.1	244	0.331	0.077	0.400	0.121	0.160
600-4	178	244	0.301	0.057	0.380	0.211	0.180
600-5	181.5	253	0.260	0.056	0.349	0.213	0.221

[a] $\Delta c_p(PB')$ = heat capacity change observed before the onset of the PEO glass transition

Then reasonable agreement is achieved with the value expected for the contribution of the polybutadiene to the overall heat capacity change at T_g. This indicates that the heat capacity change observed below the polyether transition is actually part of the polybutadiene transition, and corresponds to that portion of the polybutadiene which is immobilized, evidently due to linkage to glassy polyether segments.

The primary conclusions obtained from these calorimetric measurements are that phase separation occurs even with very short polyether chains linked to polybutadiene, and that a considerable fraction of the polybutadiene is part of an interphase of reduced mobility. However, it remains to be answered what exactly is the multiphase morphology in these systems.

Stress–strain experiments

Results. The stress–strain curves of both sets of networks are presented in *Figures 5a* and *5b*. The maximum strain to break is of the order of $\lambda = 2$. Samples were stretched up to values of $\lambda = 1.6$. *Figures 6a* and *6b* present the corresponding Mooney–Rivlin plots of the

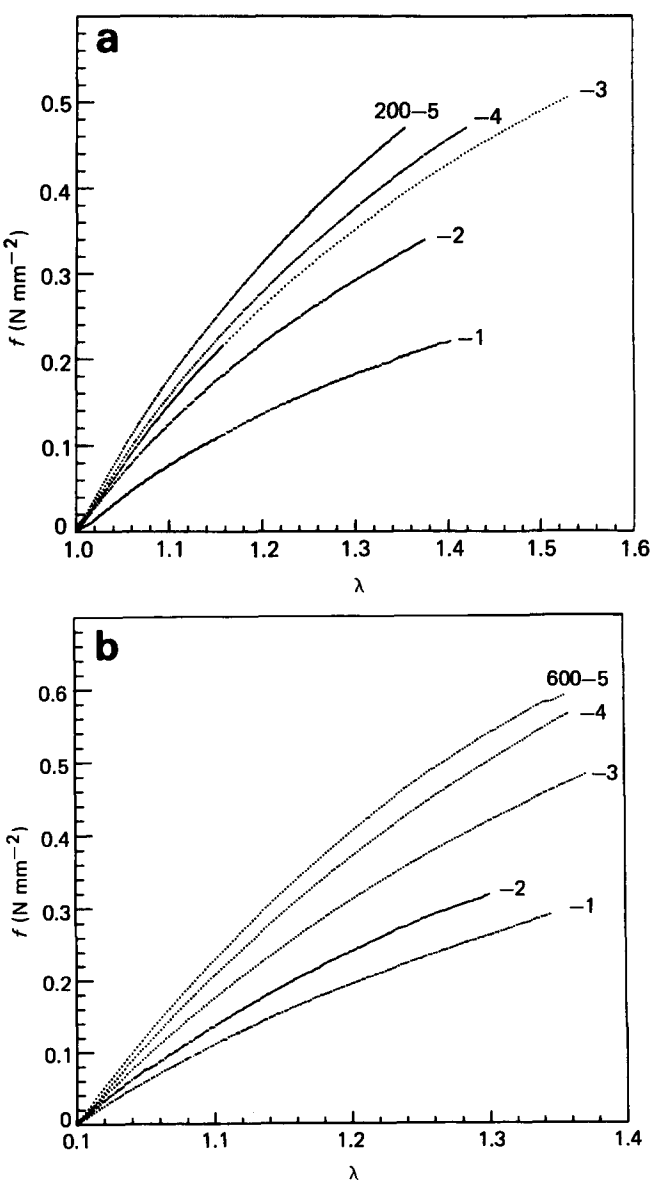

Figure 5 Stress–strain curves for the PEO-*l*-PB two-component networks: (a) series 200-*i*; (b) series 600-*i*

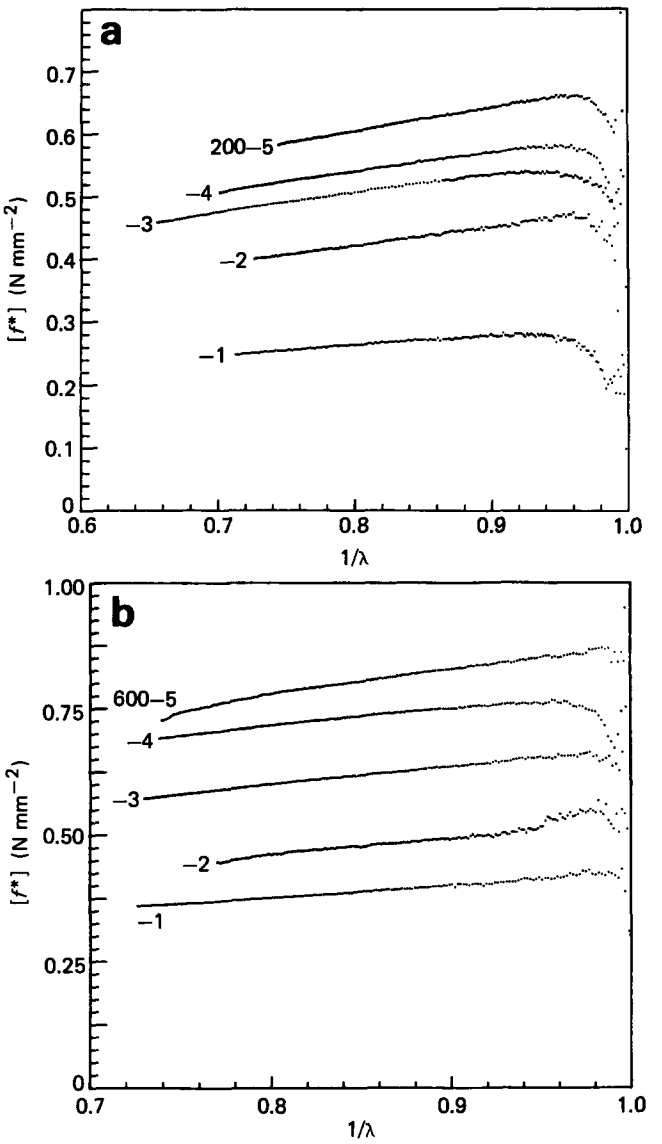

Figure 6 Mooney–Rivlin plots for the PEO-*l*-PB two-component networks: (a) series 200-*i*; (b) series 600-*i*

Table 4 Results of the stress–strain measurements

Sample	E (N mm^{-2})	$2C_1+2C_2$ (N mm^{-2})
200-1	0.82	0.29
200-2	1.23	0.48
200-3	1.50	0.56
200-4	1.67	0.59
200-5	1.95	0.67
600-1	1.18	0.42
600-2	1.49	0.51
600-3	1.83	0.67
600-4	2.09	0.78
600-5	2.43	0.87

reduced force $[f^*] = f/(\lambda - 1/\lambda^2)$ *versus* the reciprocal value of the strain.

As expected for rubbery networks, the elastic retractive force increases with increasing crosslink density. *Table 4* compares the Young's moduli obtained from the initial slope in the stress–strain experiment with the sum $(2C_1 + 2C_2)$ obtained from the Mooney–Rivlin plots. The ratio is close to one-third, as predicted by rubber elasticity theory.

Analysis of the crosslink dependence of the modulus. The initial modulus E is plotted *versus* the crosslink density in *Figure 7*, with the straight line calculated according to:

$$E = 3\rho RT/M_c = 3N_c kT \quad (1)$$

where ρ is density, $R = 8.314\,\mathrm{J\,mol^{-1}\,K^{-1}}$, $T = 298\,\mathrm{K}$, and N_c is number of elastically effective chains/cm^3. N_c was taken as twice the number of crosslinks per unit volume, as would be the case for a tetrafunctional crosslink, neglecting the occurrence of dangling chain ends or loop formation. A similar plot can be made for $2C_1 + 2C_2$ with the same result. That is, (a) there appears to be reasonable agreement between the experimental data and the simple theory of rubber elasticity based on fixed non-fluctuating crosslink junctions, and (b) the moduli of series 600-*i* are slightly larger than those of series 200-*i*.

The quite good agreement between experimental data and the values calculated according to the affine theory of rubber elasticity[12,13] is surprising considering the experimental results obtained for crosslink reactions of corresponding low-molecular-weight crosslinkers[14] obtained under similar conditions (5% concentration, room temperature). In these networks, the experimental moduli were much less than expected from the number of crosslinks. This result was explained by the formation of a large number of elastically ineffective small loops in the solution crosslink process. In addition, it was recently demonstrated that a flexible low-molecular-weight crosslinker favours the formation of small loops and reduces the crosslink efficiency[15].

Similarly, one would not expect a reduction of loop formation if a polymeric (or oligomeric) crosslinker is used. In addition, the experimental finding that the series 600-*i* moduli are higher than those of series 200-*i* must be explained.

At room temperature, both polymer components are above T_g. While the glass transition of the polybutadiene is at about −90°C, the polyether transition is only slightly below room temperature. Thus, the PEO modulus will be higher than the modulus of the polybutadiene phase. Consequently, two effects should be observed in the phase-separated two-component networks.

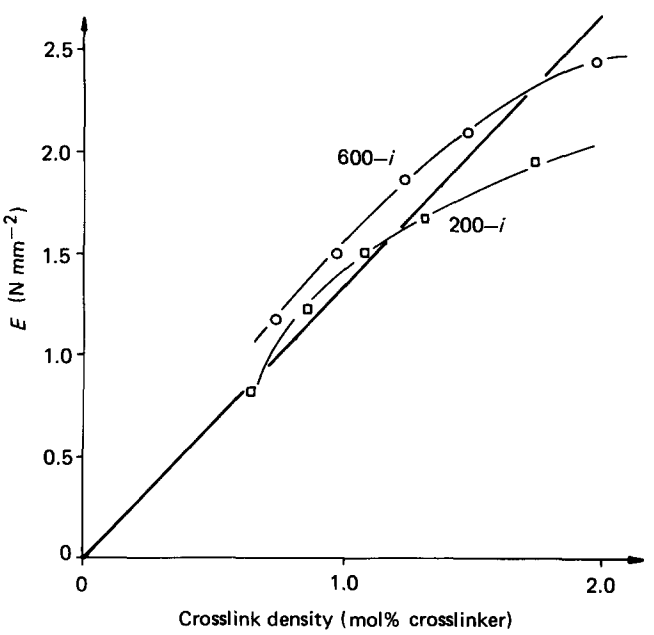

Figure 7 Young's modulus E for the PEO-*l*-PB two-component networks as a function of the crosslink density: □, series 200-*i*; ○, series 600-*i*; straight line calculated according to equation (1)

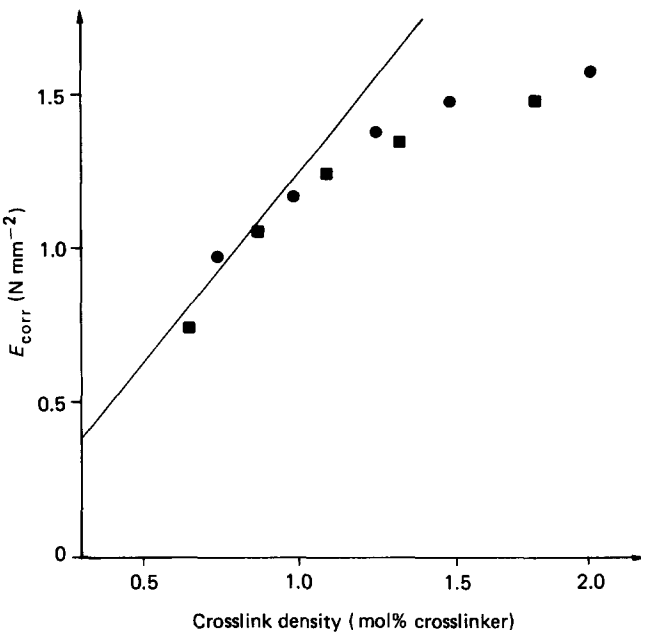

Figure 8 Young's modulus E_{corr} corrected for the weak filler effect of the PEO phase according to the Kerner model[17–19] using $E^{PEO} = 5E^{PB}$: ■, series 200-*i*; ●, series 600-*i*; straight line calculated according to equation (1)

First, the modulus should increase with increasing crosslink density. Secondly, although the PEO is above its T_g, it should act as a plastic filler and thus increase the modulus. This effect should be more pronounced in the 600-*i* series than in the 200-*i* series and is in accordance with the experimental results.

The effect of the filler on the mechanical properties can be taken into account by a two-phase mechanical model, such as the models of Takayanagi[16] or Kerner[17]. If Kerner's approach is used according to the treatment given by Faucher[18] and our previous work[19], the modulus data of both series corrected for the effect of the 'filler' are represented by the same curve (*Figure 8*). In this calculation, the PEO modulus was reasonably assumed to be approximately 5 times that of the polybutadiene. The picture does not change seriously if this factor is increased to 10.

The remaining 'filler-corrected' network modulus is lower than that calculated by the chemical stoichiometry according to the theory of rubber elasticity, probably due to the formation of loops in the solution crosslinking process. A rough estimate of the crosslink efficiency from the corrected data is 0.43 ± 0.2, which is close to the result obtained for the low-molecular-weight crosslinkers (0.33)[14].

With the restrictions imposed by the preceding discussion, the stress–strain data support the d.s.c. results of a phase-separated two-component network. The additional following remark must be added to the stress–strain results. In the two-component networks, the constants $2C_2$ in the Mooney–Rivlin equation are smaller than those of the solution crosslinked networks using a low-molecular-weight crosslinker. Rehage and Oppermann[20] showed that for poly(dimethyl siloxane) (PDMS)

networks, $2C_2$ decreases with increasing functionality. This result was explained by a decrease in the junction fluctuations in this type of network. A similar interpretation may be valid for the present two-component networks. That is, while a single PEO crosslinker may be considered either as a tetrafunctional crosslink or as two trifunctional crosslinks, phase separation would cause the formation of an apparently higher functionality and hinder the fluctuation of the junction, which would be located near the phase boundary.

Swelling experiments

It is not the purpose of this paper to give a quantitative thermodynamic description of the ternary system upon swelling the two-component networks. Swelling experiments were performed in order to gain information on the topology and morphology of the PEO-*l*-PB two-component networks. This discussion will be restricted to the swelling ratio, q, defined as $q = V/V_0$, where V is the volume of the swollen gel and V_0 is the initial volume of the dry network. Swelling measurements were performed using THF as a good solvent for both polymer components, cyclohexane as a good solvent for polybutadiene but non-solvent for the poly(ethylene oxide) chains, and water as a solvent for the polyether and non-solvent for polybutadiene. The swelling behaviour in water is especially important because the use of such hydrophilic–hydrophobic two-component networks as functional polymers, as outlined in the introduction, depends on their behaviour towards aqueous solutions. The primary subjects to be addressed by the swelling experiments are:

(a) the dependence of the degree of swelling on the crosslink density, and

(b) the influence of polyether chain length and crosslink density on swelling by water.

Swelling in THF and cyclohexane. Because THF is a good solvent for both polymer components, the equilibrium degree of swelling should be a measure of the crosslink density, and any tendency to phase-separate should be minimized. *Figure 9* plots q (equilibrium degree of swelling) as a function of the crosslink density at 20°C in THF. As expected, q decreases with increasing crosslink density. At equivalent crosslinker concentrations, the networks with the longer polyether chains swell to a slightly higher degree, which may indicate that THF favours the solvation of the PEO chain over that of polybutadiene.

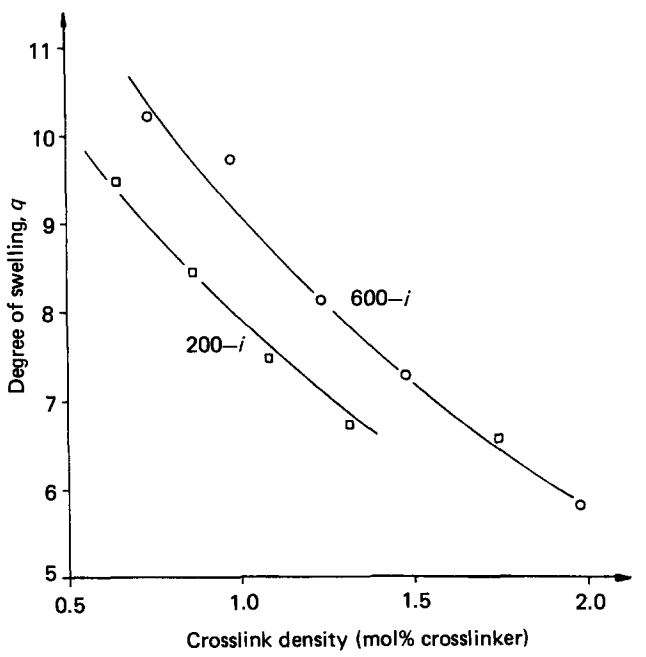

Figure 9 Equilibrium degree of swelling for the two-component networks in THF at 20°C: □, series 200-*i*; ○, series 600-*i*

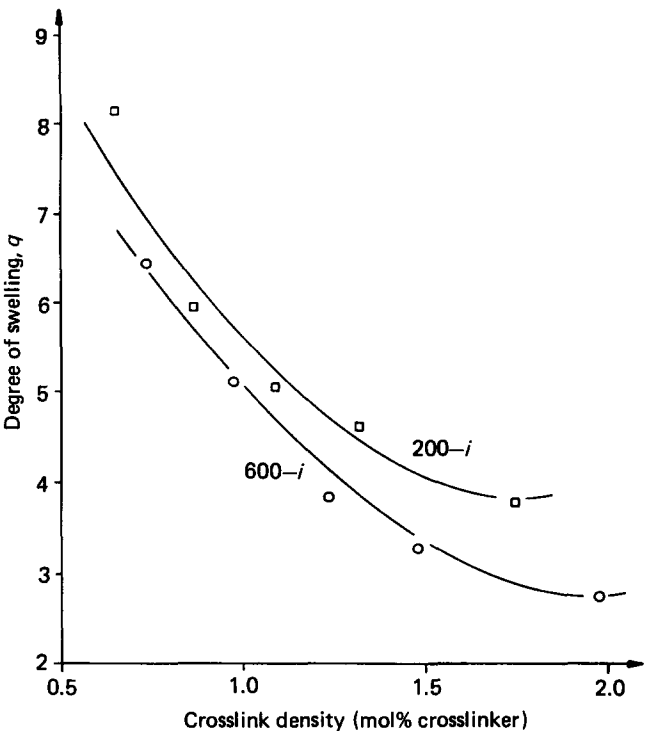

Figure 10 Equilibrium degree of swelling for the two-component networks in cyclohexane at 20°C: □, series 200-*i*; ○, series 600-*i*

In *Figure 10*, q is plotted for two network series in cyclohexane. As in the case of THF, q decreases with increasing crosslink density. These values of q are lower than those obtained using THF. The most significant observation is that, in contrast to the results in THF, series 600-*i* have a lower degree of swelling in cyclohexane than do series 200-*i*. This reflects that there is a higher fraction of PEO in series 600-*i* and that the polyether chains will not swell at all or only to a low degree in cyclohexane. The swelling may also depend on the phase morphology if phase separation persists in the swollen gels.

Swelling behaviour in water. The results of the equilibrium swelling of series 200-*i* and 600-*i* in water are shown in *Figure 11*, and represent the average of three samples each. The error bars indicate the estimated maximum error. Three significant experimental observations must be discussed. First, both series swell considerably in water. Secondly, the series 600-*i* q values are larger than those of 200-*i*. Thirdly, swelling by water shows a maximum at intermediate crosslink densities.

Because all networks swelled in water even when the polybutadiene was present in large excess, the polyether chains cannot form isolated domains embedded in the polybutadiene matrix, but rather must form an interconnected structure.

To substantiate this assumption, a preliminary electron microscopic study on an OsO_4-stained 200-3 sample (i.e.

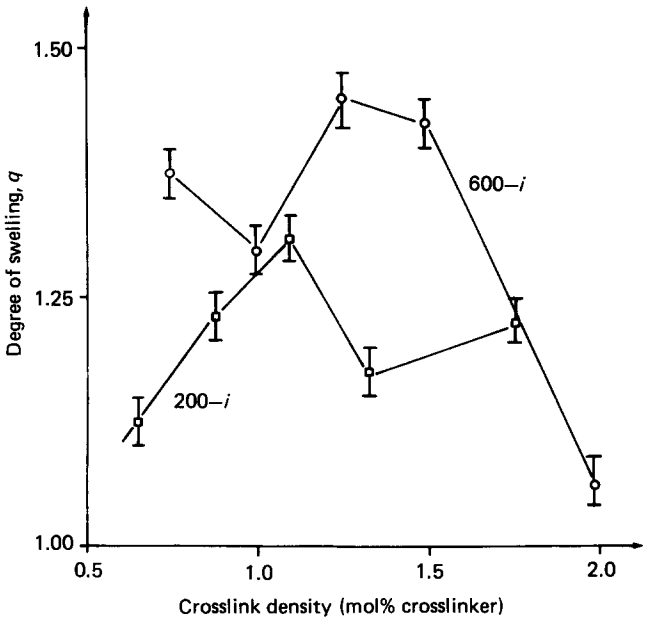

Figure 11 Equilibrium degree of swelling for the two-component networks in water at 20°C: □, series 200-*i*; ○, series 600-*i*

the network with the short polyether with the maximum water swellability) was performed*. *Figure 12a* shows the structure observed in the transmission micrograph. In a dark matrix, stained PB, the polyether phase forms a continuous structure of interconnected channels. The diameter of these channels is of the order of 2–4 nm. Including the heterocyclic end groups, the length of the fully extended polyether chain is 4.0 to 4.5 nm if the number-average chain length is used.

The bicontinuous morphological network of PB and PEO is shown schematically in *Figure 12b*. This bicontinuous morphology resembles structures occurring in the initial steps of a spinodal demixing process. The reason for this structural similarity may be that the crosslink reaction is performed in THF where a more or less homogeneous reaction mixture is formed. Upon solvent evaporation, demixing begins, but it is limited by the chemical network topology. The size of the polyether phase is thus limited by fixation of both chain ends to polybutadiene.

Variation of the hydrophilic–hydrophobic balance. The occurrence of a maximum in the equilibrium degree of swelling in water at medium crosslink densities and the different behaviour of series 200-*i* and 600-*i* reflect the sensitivity of such two-component networks to the hydrophobic–hydrophilic balance. With increasing crosslink density, the mass fraction of hydrophilic polyether increases. On the other hand, the increase of the crosslink density will decrease the swellability of the system. These opposing effects are responsible for the swelling maximum and can be treated separately by normalization to a convenient reference state.

The influence of increasing crosslink density, independent of the crosslinker's chain length, can be eliminated by using swelling in THF as a reference state. As discussed above, both polymers are readily soluble in THF. Thus, the decrease of q in THF reflects the increasing crosslink density. The relative swelling q_r, defined as the ratio q_{water}/q_{THF}, eliminates the effects of crosslinking, and is plotted as a function of the weight fraction of hydrophilic crosslinker in *Figure 13*. Both series can be represented by a single curve showing the increasing water uptake with increasing polyether content.

On the other hand, the influence of increasing crosslink

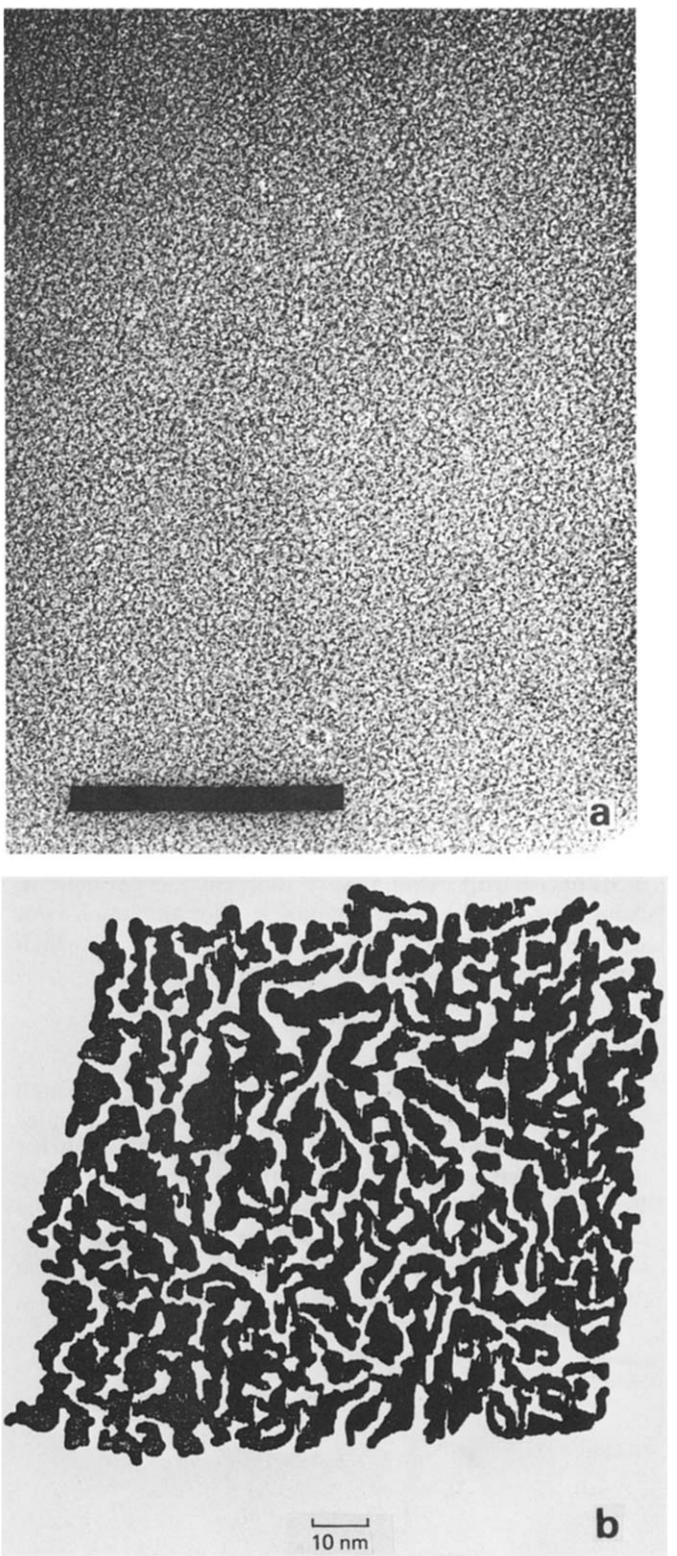

Figure 12 (a) Transmission electron micrograph of network 200-3, stained by OsO_4. Bar is 0.2 μm. (b) Schematic picture of the bicontinuous morphology of the PEO-*l*-PB two-component network

* The authors are indebted to M. Kunz for performing the electron microscopic investigation on the Zeiss Electron Microscope 904 in the elastic bright-field mode (Electron Microscopy Laboratory of the Sonderforschungsbereich 60)

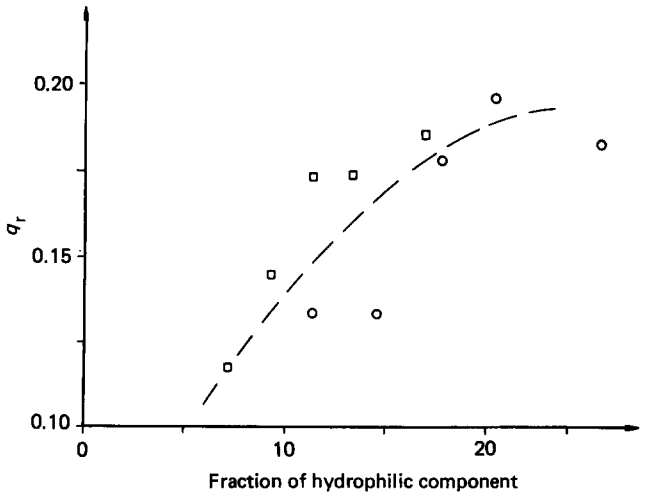

Figure 13 Relative swelling $q_r = q_{water}/q_{THF}$ as a function of the weight fraction of crosslinker: □, series 200-*i*; ○, series 600-*i*

density can be considered with reference to the ratio of the degree of swelling in water to the amount of hydrophilic component in the network. In *Figure 14*, q_H, defined as q_{water}/(wt% crosslinker), is plotted *versus* the crosslink density. As expected, the relative water swellability decreases with increasing crosslink density. Again a single curve is obtained for both series of networks.

CONCLUSIONS

Well defined PEO-*l*-PB two-component networks were prepared. Phase separation occurred in these systems even when very short polyether chain lengths were used. Owing to the network-forming reaction in solution, a morphological network consisting of two bicontinuous phases were formed. The structure of the network influences both the mechanical and swelling behaviour. The results of swelling in water showed that the hydrophilic–hydrophobic balance in such systems is sensitive to the length of the polyether chains and the crosslink density. Preliminary data on the permeation behaviour towards aqueous media show that such two-component networks have interesting properties, which might be exploited for membrane applications[21].

ACKNOWLEDGEMENTS

This work has been supported by the AIF through Project 6997 and by the Schwerpunkt 29 des Landes Baden-Württemberg (Zeiss ELMI 904). M.W. acknowledges a fellowship through the Graduiertenkolleg Polymerwissenschaften der Universität Freiburg. The authors are indebted to M. Kunz for taking the electron microscopic pictures and to C. Pugh for revising the manuscript.

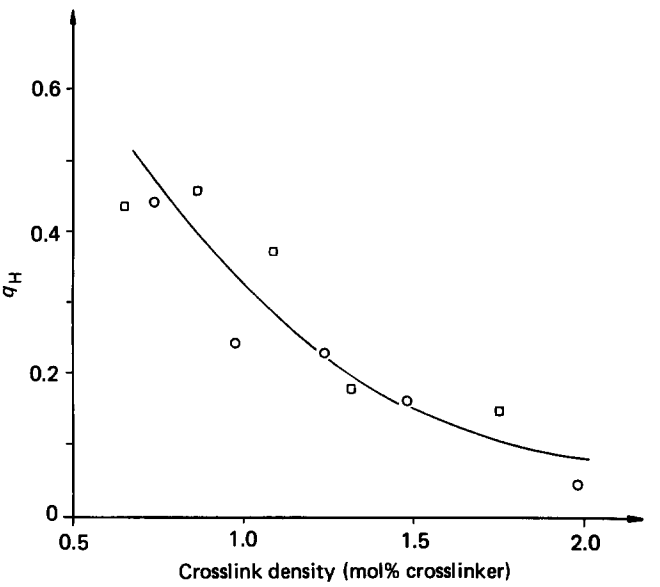

Figure 14 Reduced degree of swelling $q_H = q_{water}$/(wt% crosslinker) as a function of the crosslink density: □, series 200-*i*; ○, series 600-*i*

REFERENCES

1 Paul, D. R. and Sperling, L. H. (Eds.), 'Multicomponent Polymer Materials', Adv. Chem. Ser. 211, American Chemical Society, Washington DC, 1986
2 Thomas, D. A. and Sperling, L. H. in 'Polymer Blends', (Eds. D. R. Paul and S. Newman), Academic Press, New York, 1978
3 Weber, M. and Stadler, R., preceding paper
4 Weber, M., Diploma Thesis, University of Freiburg, 1986
5 Butler, G. B. *Ind. Eng. Chem., Prod. Res. Dev.* 1980, **19**, 512
6 Leong, K. W. and Butler, G. B. *J. Macromol. Sci., Chem.* 1980, **14**, 287
7 de Lucca Freitas, L., Maldaner Jacobi, M. and Stadler, R. *Polym. Bull.* 1984, **11**, 407
8 Stadler, R., de Lucca Freitas, L. and Maldaner Jacobi, M. *Makromol. Chem.* 1986, **187**, 723
9 Bühler, F., Stadler, R. and Gronski, W. *Makromol. Chem.* 1986, **187**, 1295
10 Ward, I. M., 'Mechanical Properties of Solid Polymers', Wiley, New York, 1971
11 Grebowicz, J., Aycock, W. and Wunderlich, B. *Polymer* 1986, **27**, 575
12 Treloar, L. R. G., 'The Physics of Rubber Elasticity', 3rd Edn., Clarendon Press, Oxford, 1975
13 Flory, P. J., 'Principles of Polymer Chemistry', Cornell University Press, Ithaca, NY, 1953
14 Stadler, R., Bühler, F. and Gronski, W. *Makromol. Chem.* 1986, **187**, 1301
15 Bica, C., Jacobi, M. M., de Araujo, M. A. and Stadler, R., in preparation
16 Takayanagi, M. S., Uemura, S. and Minami, S. *J. Polym. Sci.* 1964, **C5**, 113
17 Kerner, E. H. *Proc. Phys. Soc. Lond.* 1956, **69B**, 808
18 Faucher, J. A. *J. Polym. Sci., Polym. Phys. Edn.* 1974, **12**, 2153
19 Stadler, R. and Gronski, W. *Colloid Polym. Sci.* 1983, **261**, 215
20 Oppermann, W. and Rehage, G. in 'Elastomers and Rubber Elasticity' (Ed. J. E. Mark), ACS Symp. Ser. 193, American Chemical Society, Washington DC, 1982, p. 309
21 Weber, M. and Stadler, R., work in progress